

List of Figure Captions

Figure 1 Several valves and the vacuum pump removed for clarity. A more detailed schematic is provided in the experimental procedure section. Gas is charged from the cylinder (S) through the pressure regulator, and into pumps P1 and P2. Gas then flows through the 24 inch equilibration column to ensure that the gas is at the bath temperature. Gas is dispersed in the saturation cell (SC) into fine bubbles (1-2 micron size), and is then reduced in pressure through throttling valves TV1 and TV2. The analytical train (denoted by the dashed box A) then receives the low pressure sample from the second throttle valve. Gas flows to either the Panametrics Moisture Analyzer (PMA) or to the desiccant packed u-tubes. Pressure in the analysis section is recorded by a pressure transducer. For the high temperature runs, a pre-saturation column (not shown) is used between P1 and P2 to ensure that the gas is completely water saturated.

Figure 2 This figure shows the internal details of the high-pressure saturation cell. The porous frit and retaining ring disperse the incoming gas into 1-2 micron bubbles, facilitating mass transfer. Cell temperature is recorded using a thermowell with a j-type thermocouple inside. Over pressure protection is provided by a 19,500 psia rupture disc, and internal pressure is measured by two pressure transducers, one 0-10,000 and one 0-20,000 depending on the pressure under investigation. The anti-entrainment baffle section is made from 304 stainless and Teflon. The O-rings were either Viton for the hydrocarbon rich mixtures, or Teflon for the carbon dioxide rich mixtures.

Figure 3 Water content of pure carbon dioxide as a function of temperature and pressure. (o): experimental data by Song and Kobayashi⁷; (Δ): experimental data by Gillespie and Wilson⁶; (\square): experimental data by King et al.⁵⁸; (\diamond): experimental data by Nakayama et al.⁵⁹; (-): PC-SAFT predictions.

Figure 4 Water content of pure hydrogen sulfide as a function of temperature and pressure. (o): smoothed data by Selleck et al.¹⁰; (Δ): experimental data by Chapoy et al.¹²; (\square): experimental data by Gillespie et al.¹¹; (\diamond): experimental data by Burgess and Germann⁶⁰; (-): PC-SAFT predictions.

Figure 5 (a) Pure nitrous oxide coexistence curve. (b) Vapor pressure of pure nitrous oxide. (o): data by Lemmon et al.⁶²; (-): PC-SAFT correlation.

Figure 6 Water content of pure nitrogen as a function of temperature and pressure. (a): experimental data by Mohammadi et al.⁶³ (all colors); (b): experimental data by Rigby and Prausnitz⁴⁸; (c): experimental data by Tabasinejad et al.⁶⁴; (–): PC-SAFT predictions.

Figure 7 Water content of argon gas as a function of temperature and pressure. (o): experimental data by Rigby and Prausnitz⁴⁸; (–): PC-SAFT predictions.

Figure 8 Water content of nitrous oxide gas as a function of temperature and pressure. (o): experimental data by Coan and King⁵⁸; (–): PC-SAFT predictions.

Figure 9 (a) Vapor-liquid equilibrium of methane + carbon dioxide mixture at 270 K. (b) Vapor-liquid equilibrium of methane + hydrogen sulfide mixture at 310.9 K. (o): experimental data^{71,72}; (–) PC-SAFT predictions with $k_{ij} = 0$; (– –) PC-SAFT predictions with a $k_{ij} = 0.046$ for Figure 9 (a) and a $k_{ij} = 0.055$ for Figure 9 (b).

Figure 10 Water content of methane + carbon dioxide mixture as a function of temperature and pressure. (o, □, Δ): experimental data; (–): PC-SAFT predictions. (a): experimental data by this work for gaseous mixture of 90 mol. % CH₄ and 10 mol. % CO₂; (b): experimental data by Sharma¹³ for gaseous mixture of 88.69 mol. % CH₄ and 11.31 mol. % CO₂; (c): experimental data by Sharma¹³ for gaseous mixture of 79.78 mol. % CH₄ and 20.22 mol. % CO₂; (d): experimental data by this work for gaseous mixture of 30 mol. % CH₄ and 70 mol. % CO₂; (e): experimental data by Song and Kobayashi⁹ for gaseous mixture of 5.31 mol. % CH₄ and 94.69 mol. % CO₂; (f): water content of methane + carbon dioxide mixture as a function of composition and pressure at 298.15 K.

Figure 11 Water content of methane + hydrogen sulfide mixture as a function of pressure at 327.59 K. (a): gaseous mixture is 91.7 mol. % CH₄ and 8.3 mol. % H₂S. (b): gaseous mixture is 82.17 mol. % CH₄ and 17.83 mol. % H₂S. (o): experimental data by Sharma¹³. (–): PC-SAFT predictions.

Figure 12 Vapor-liquid equilibrium of carbon dioxide + hydrogen sulfide system at 313.02 K. (o): experimental data⁷³; (—) PC-SAFT predictions with a $k_{ij} = 0$; (— —) PC-SAFT predictions with a $k_{ij} = 0.062$.

Figure 13 Water content of carbon dioxide + hydrogen sulfide mixture as a function of pressure at 333.15 K and 363.15 K. (a): gaseous mixture is 80 mol. % CO₂ and 20 mol. % H₂S. (b): gaseous mixture is 50 mol. % CO₂ and 50 mol. % H₂S. (o, □): experimental data by Clark⁸; (—) PC-SAFT predictions.

Figure 14 Phase boundaries and pressure-temperature conditions for natural gas mixture. (Δ): VLE dew point of the mixture; (□): VLLE dew point of the mixture; (o): VLLE bubble point of the mixture; experimental data by Huang et al.⁷⁵; (—) PC-SAFT predictions.

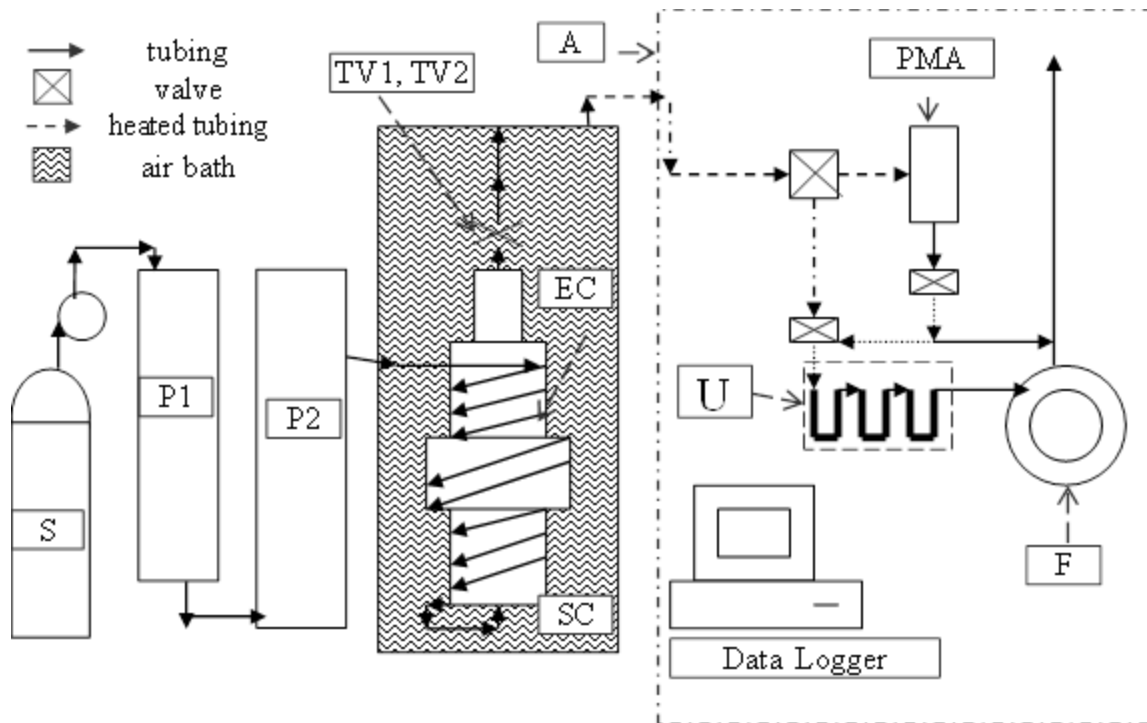


Figure 1

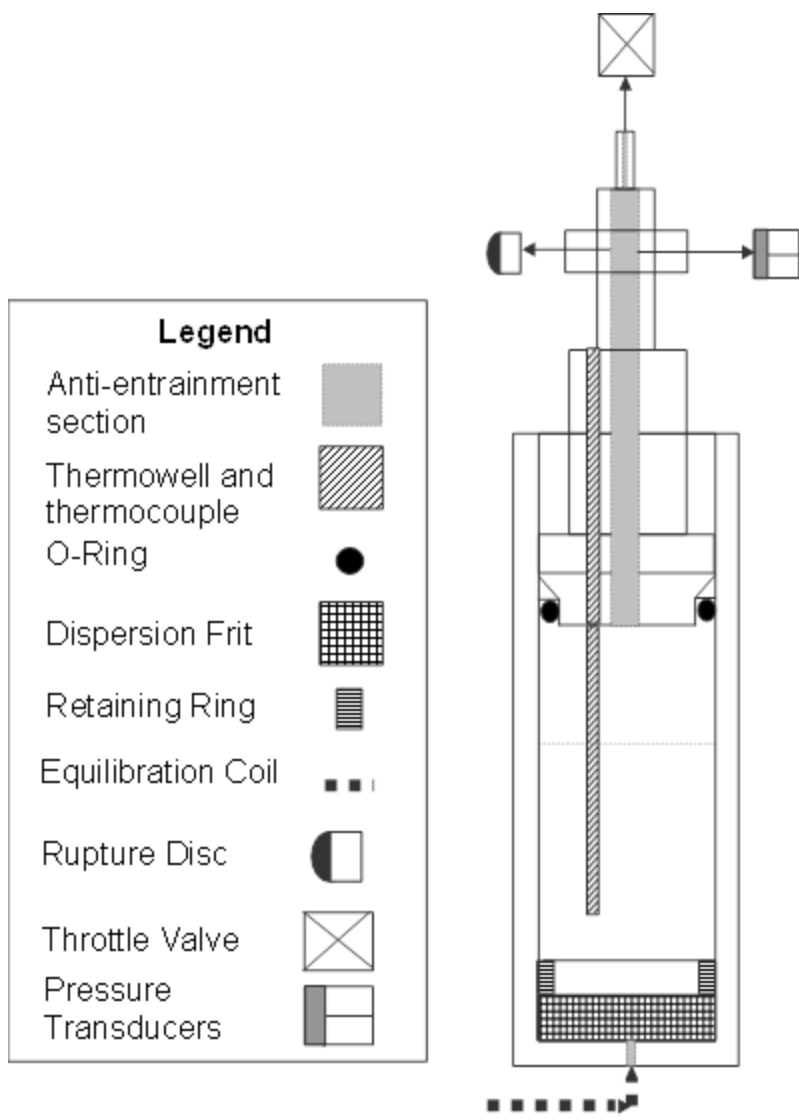
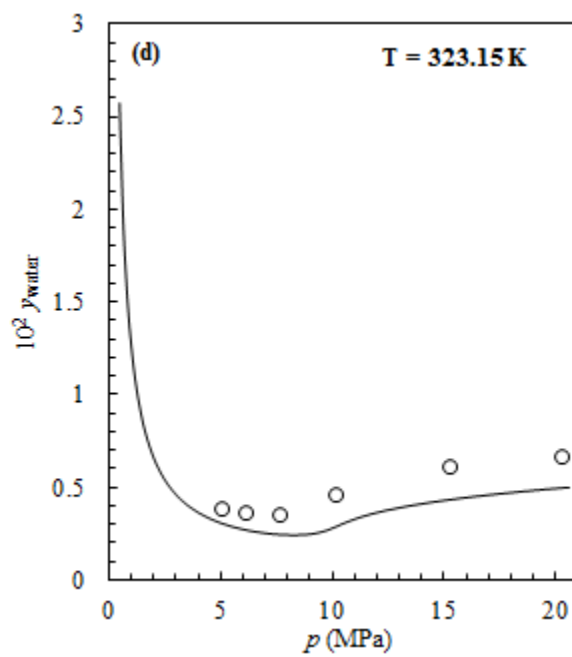
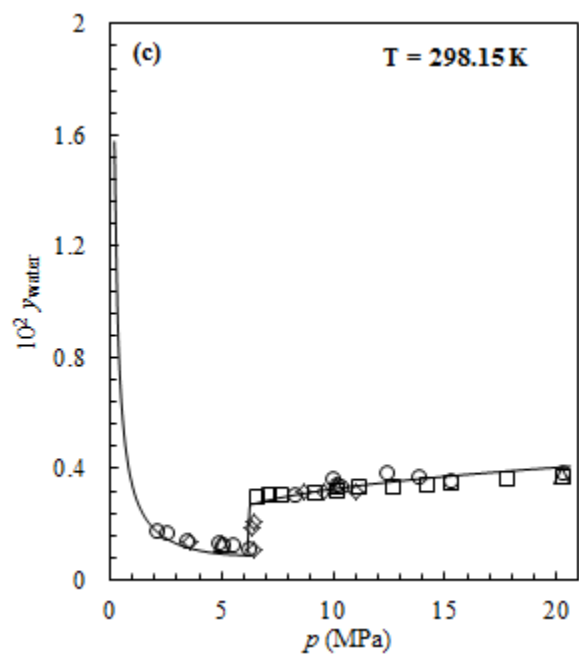
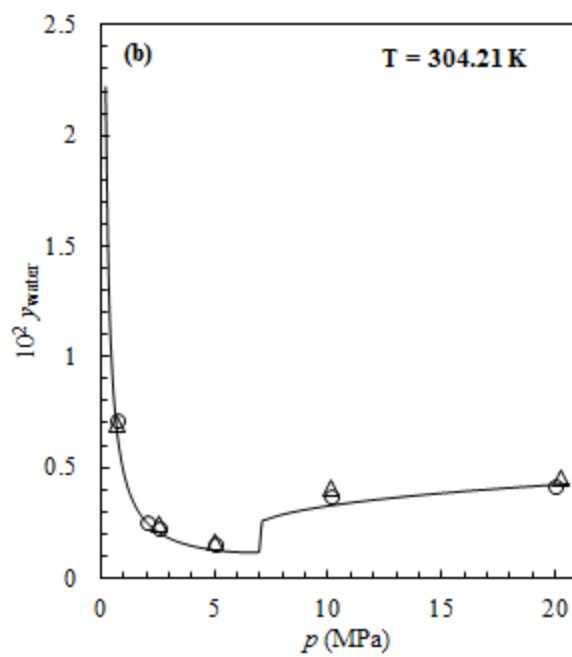
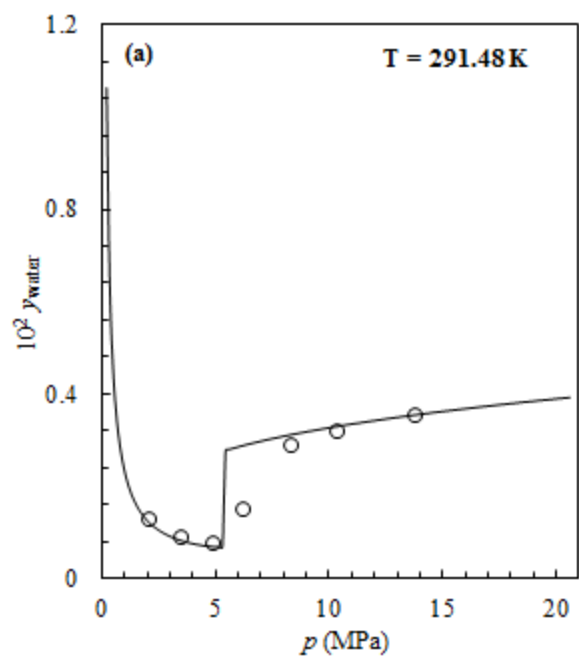


Figure 2



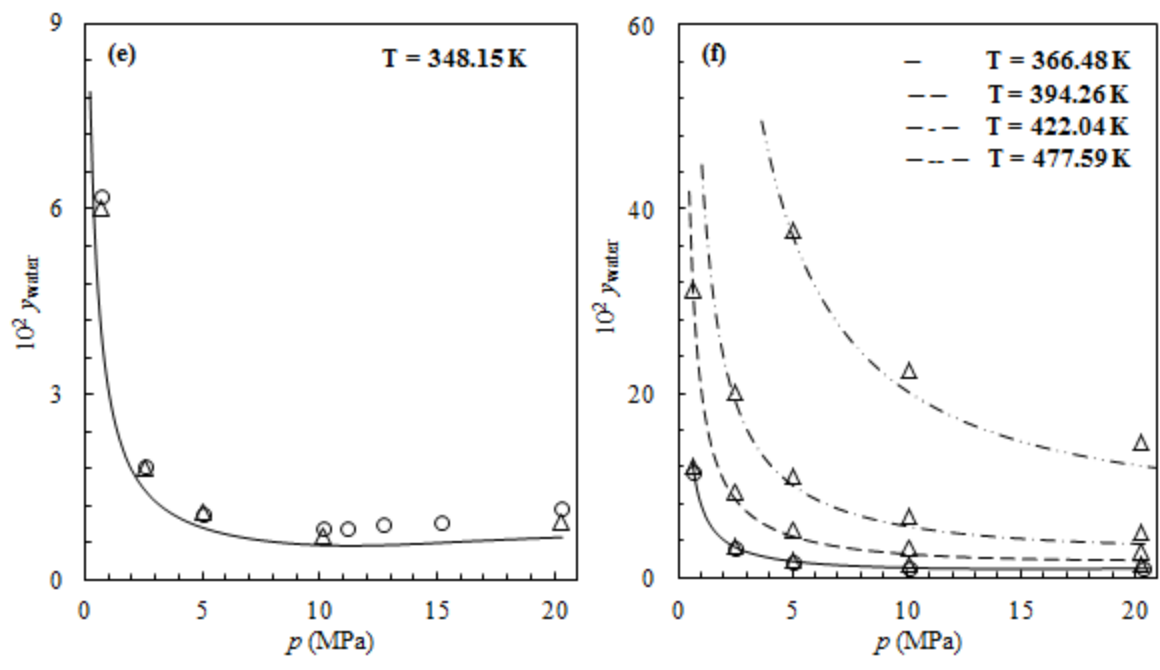
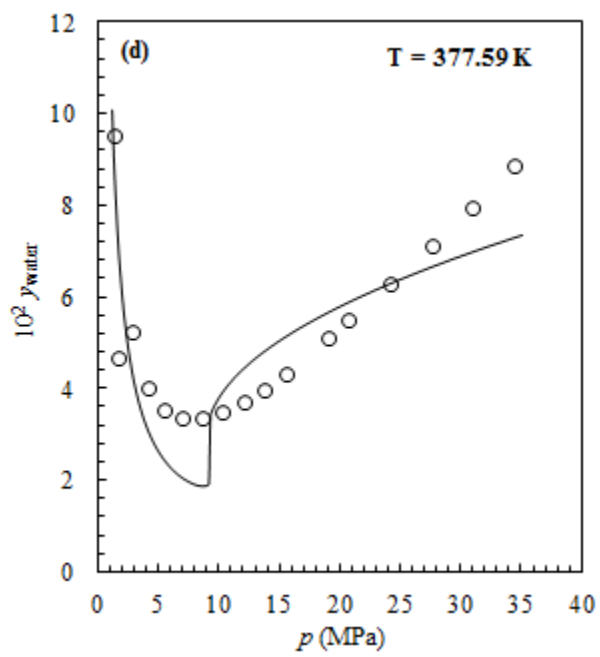
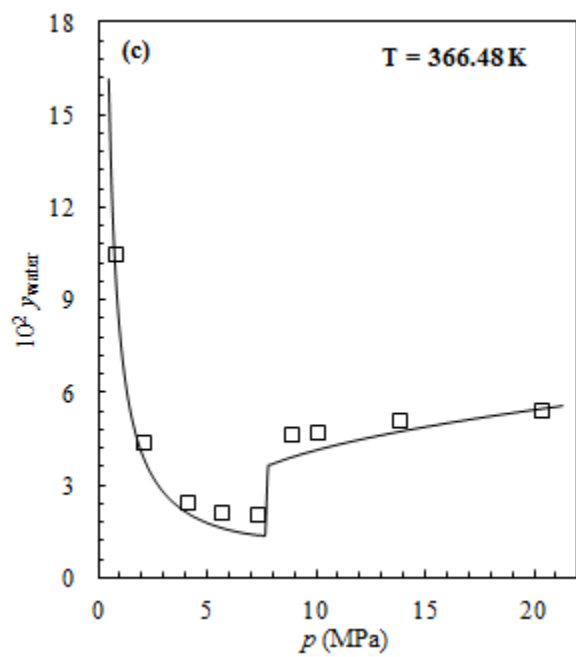
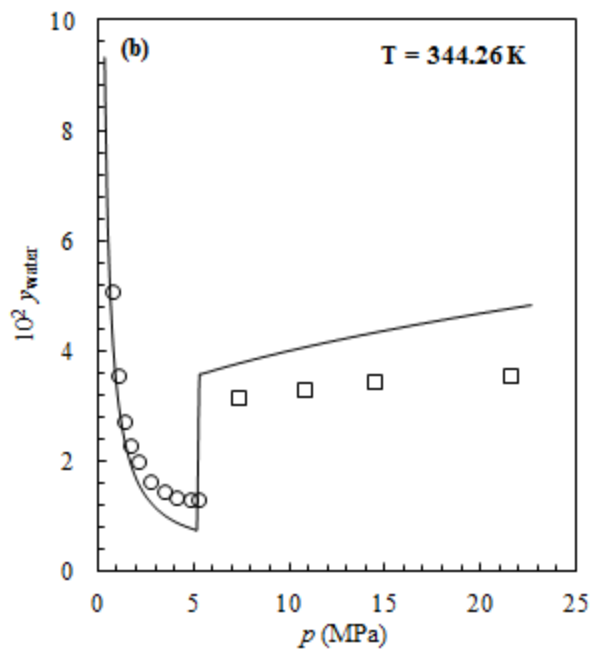
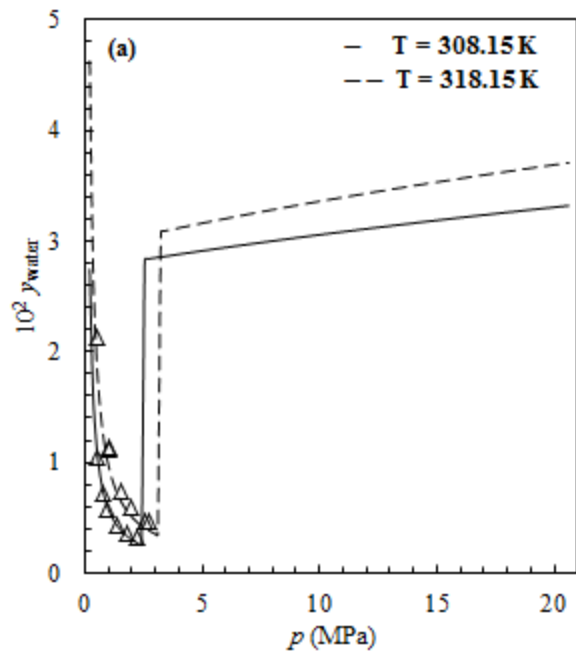


Figure 3



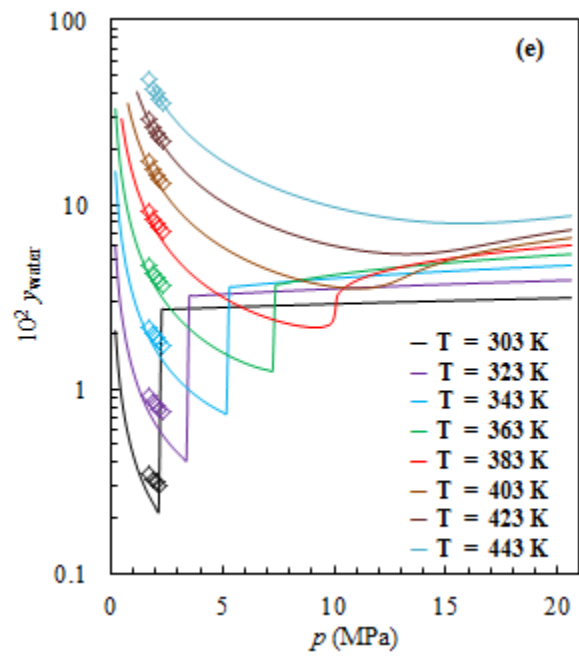


Figure 4

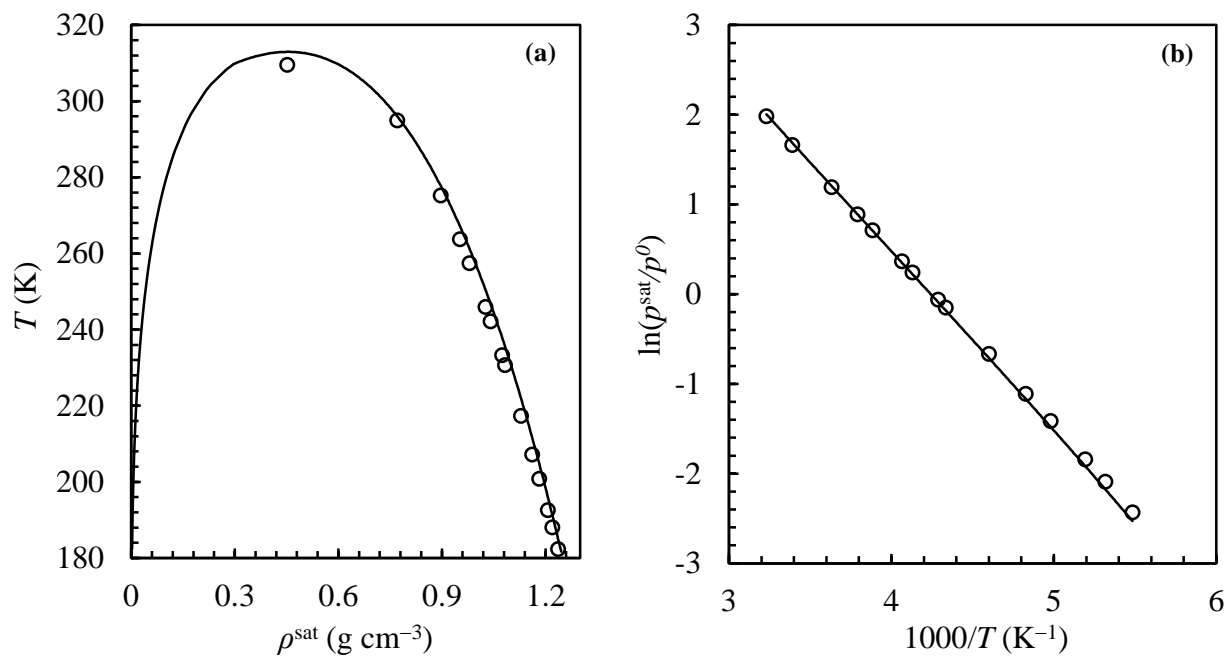


Figure 5

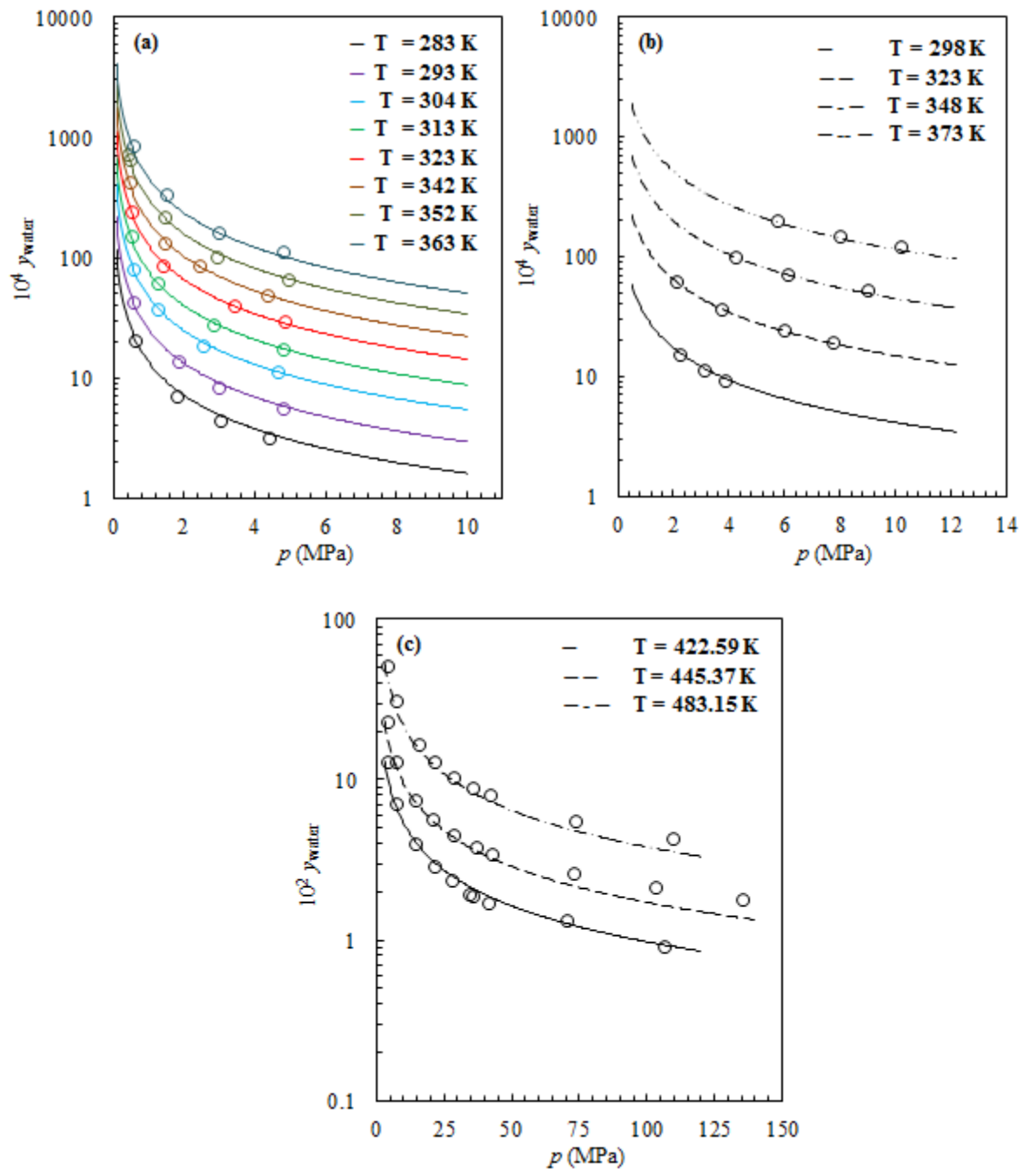


Figure 6

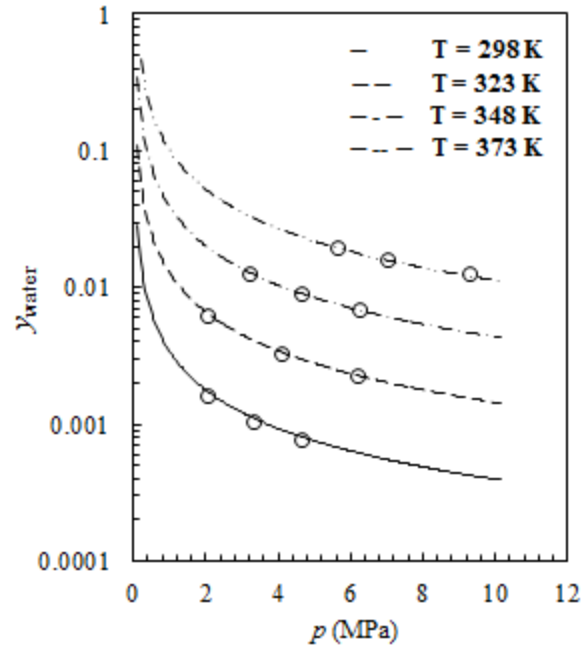


Figure 7

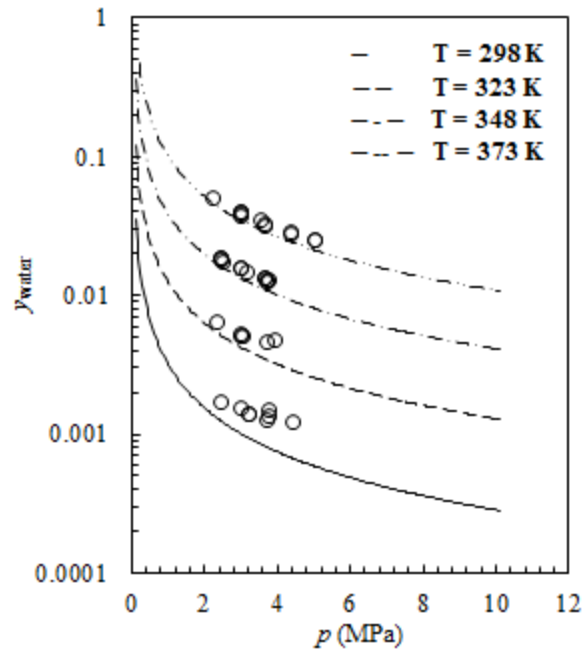


Figure 8

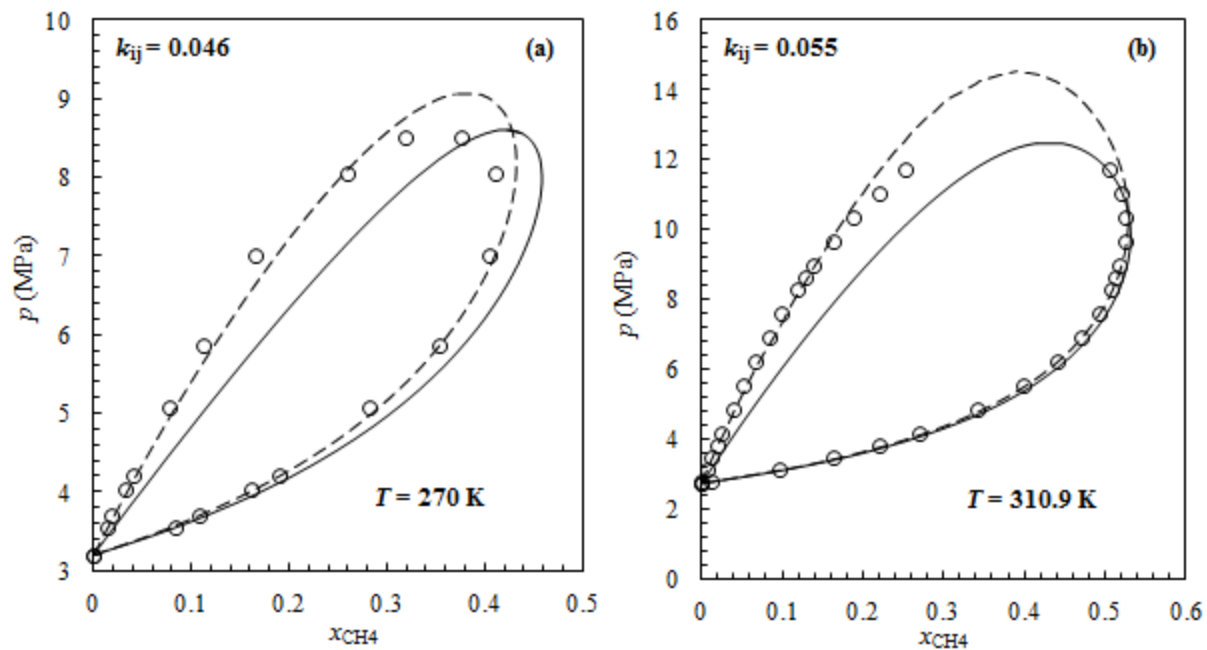
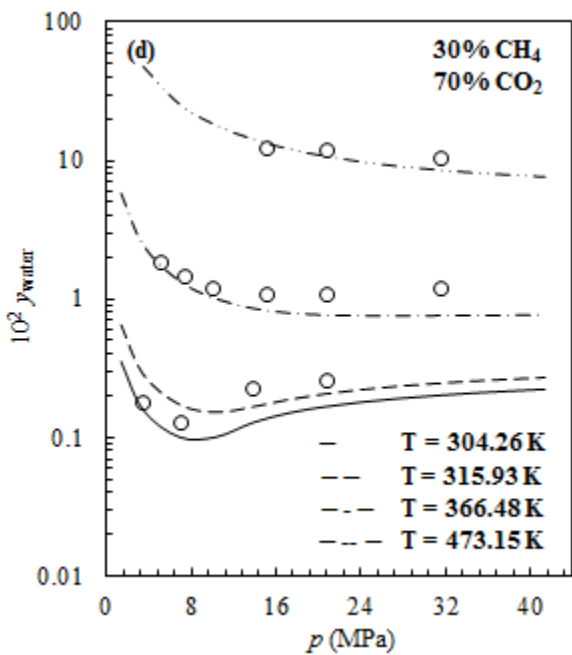
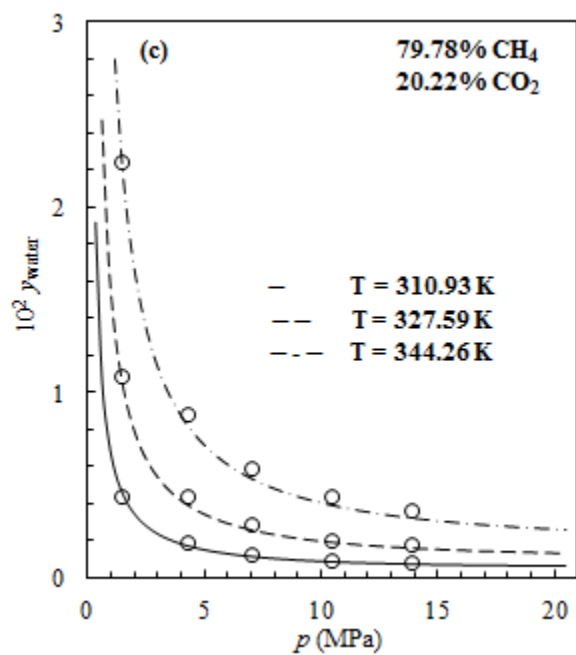
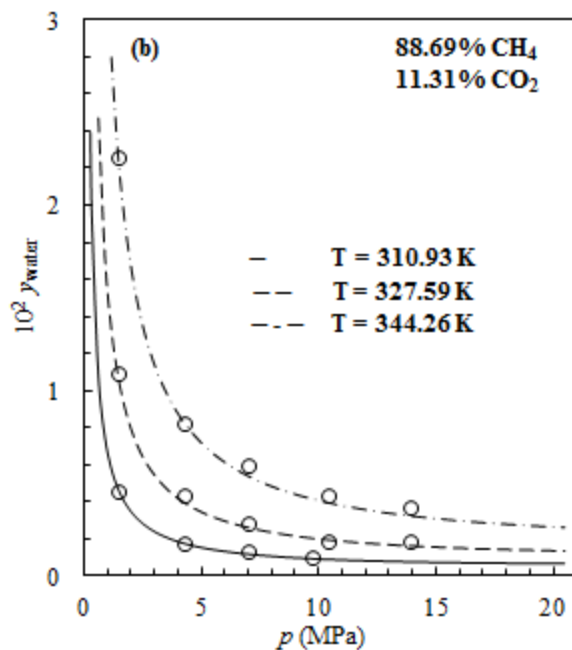
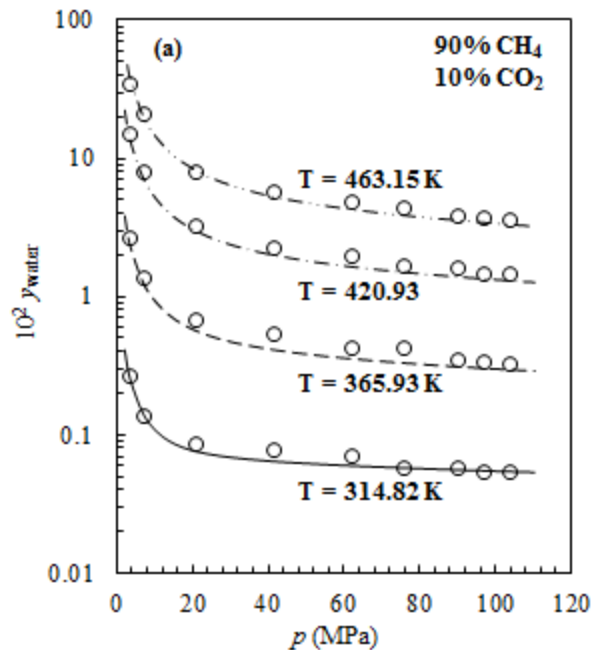


Figure 9



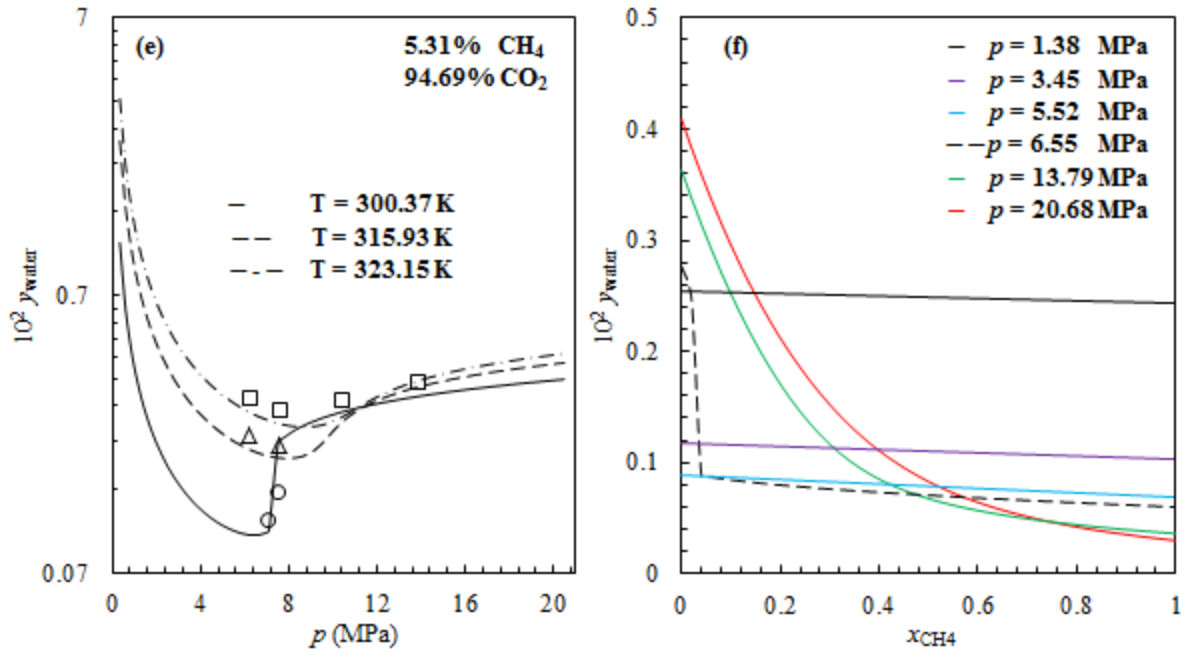


Figure 10

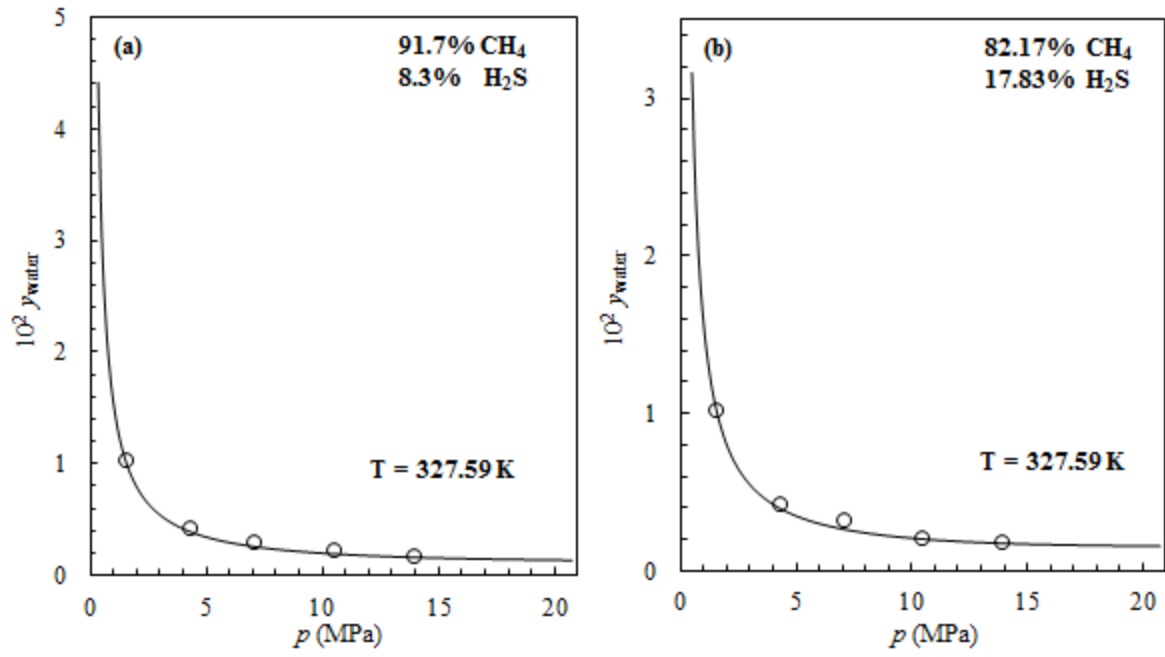


Figure 11

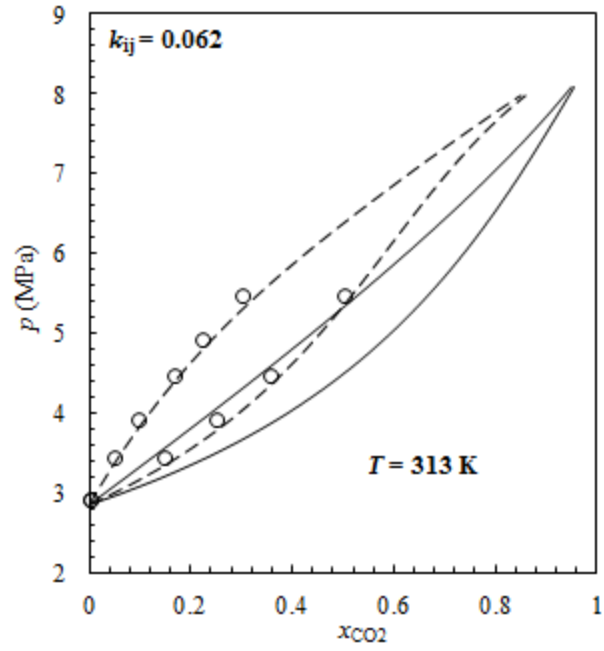


Figure 12

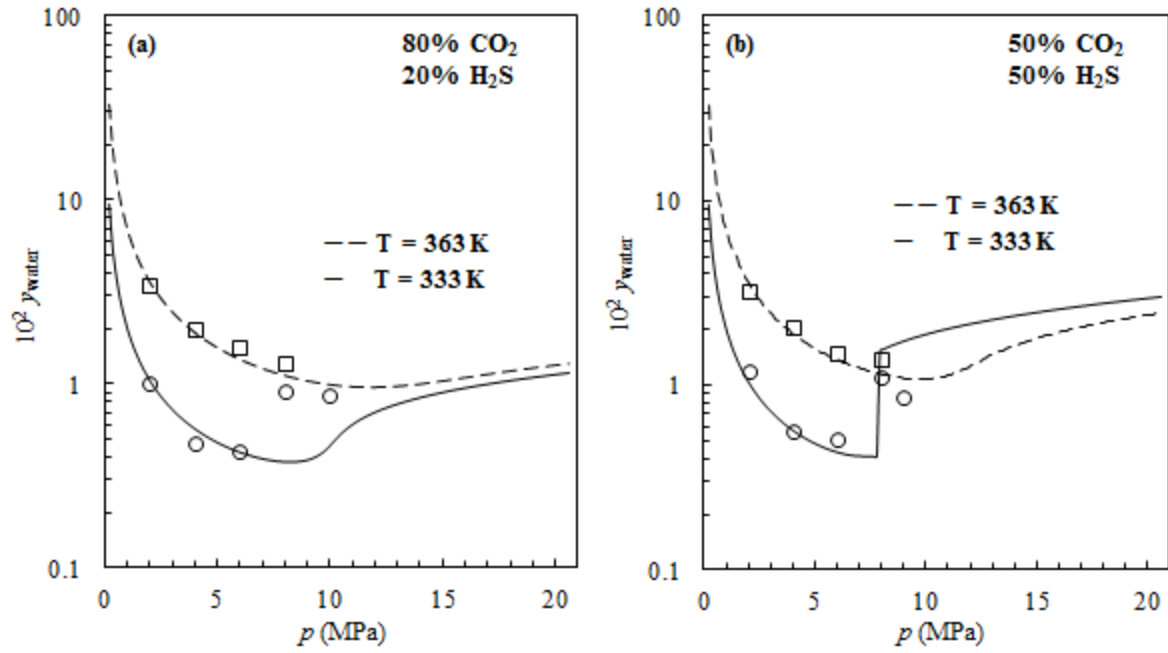


Figure 13

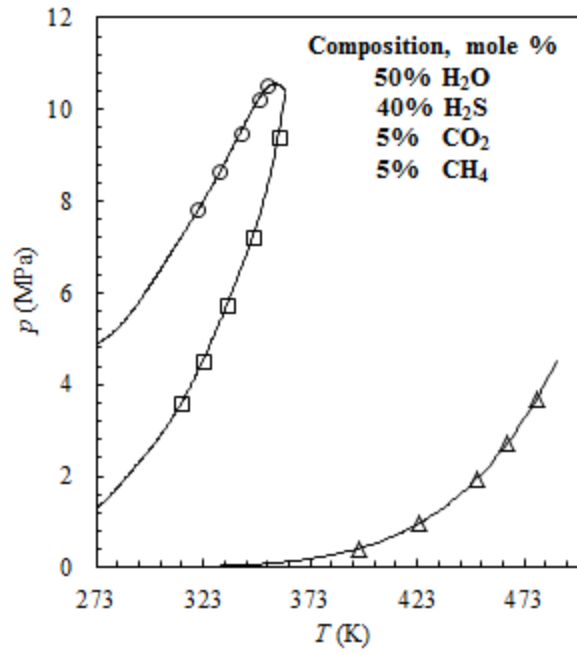


Figure 14